
Title: An EEG-EMG Correlation-based Brain-Computer Interface for Hand Orthosis Supported Neuro-Rehabilitation

Author: Anirban Chowdhury Haider Raza Yogesh Kumar Meena Ashish Dutta Girijesh Prasad

PII: S0165-0270(18)30379-0
DOI: https://doi.org/doi:10.1016/j.jneumeth.2018.11.010
Reference: NSM 8186

To appear in: *Journal of Neuroscience Methods*

Received date: 24 July 2018
Revised date: 11 November 2018
Accepted date: 14 November 2018

Please cite this article as: Anirban Chowdhury, Haider Raza, Yogesh Kumar Meena, Ashish Dutta, Girijesh Prasad, An EEG-EMG Correlation-based Brain-Computer Interface for Hand Orthosis Supported Neuro-Rehabilitation, *<![CDATA[Journal of Neuroscience Methods]]>* (2018), https://doi.org/10.1016/j.jneumeth.2018.11.010

Article Type: Research Paper

Title: An EEG-EMG Correlation-based Brain-Computer Interface for Hand Orthosis Supported Neuro-Rehabilitation

Authors:
Anirban Chowdhury[a], Haider Raza[b], Yogesh Kumar Meena[c], Ashish Dutta[a], Girijesh Prasad[d]

[a]Centre of Mechatronics, Indian Institute of Technology, Kanpur, India
[b]School of Computer Science and Electronic Engineering, University of Essex
[c]Department of Computer Science, Swansea University
[d]School of Computing and Intelligent Systems, Ulster University

*corresponding author.

Anirban Chowdhury
Centre for Mechatronics,
Department of Mechanical Engineering,
IIT Kanpur, Kanpur,
India, PIN-208016.
email: anir@iitk.ac.in

**Highlights:**

1. BCI system based on EEG-EMG correlation between band-limited power time-courses, is developed.
2. The proposed method of achieved 92.81±2.01% accuracy in healthy subjects.
3. The accuracy was 84.53±4.58% in case of stroke patients.
4. The accuracy of CBPT was higher ($p<0.05$) than the corticomuscular coherence method.
5. CBPT has the potential to be used for corticomuscular interaction based neurorehabilitation.

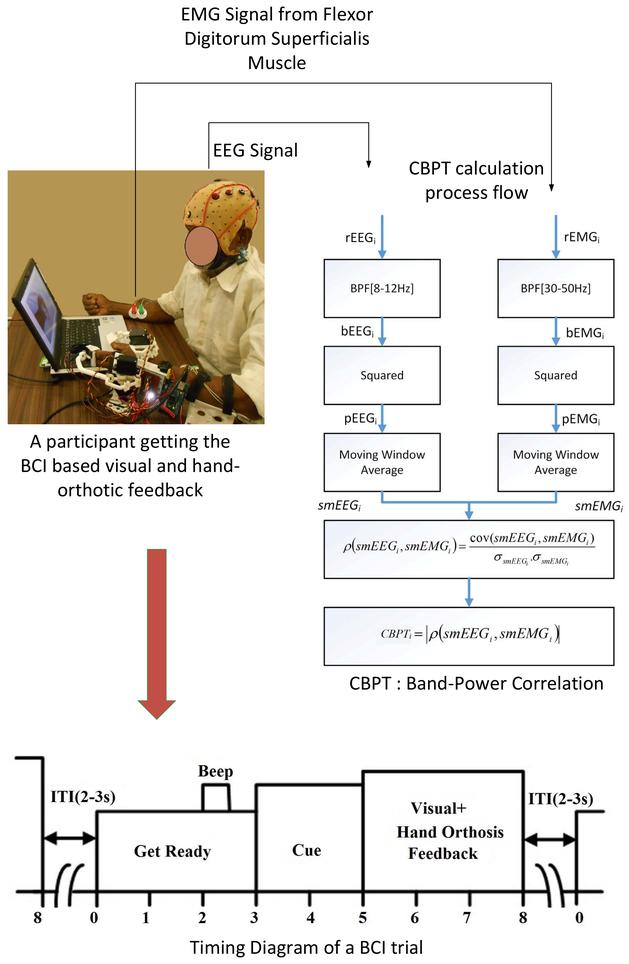


A participant getting the BCI based visual and hand-orthotic feedback

Timing Diagram of a BCI trial

EEG and EMG Signal Transformation during CBPT calculation

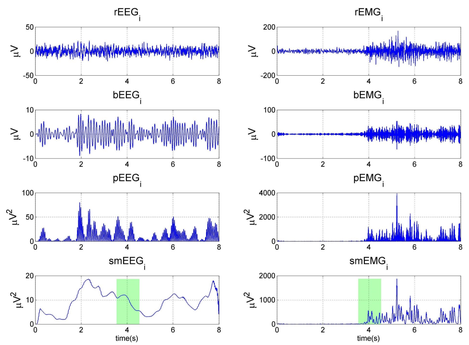


Comparison between CMC and CBPT based BCI

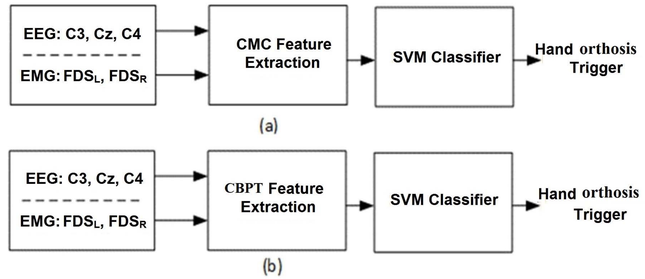


CBPT Feature Separation between Left and Right hand tasks

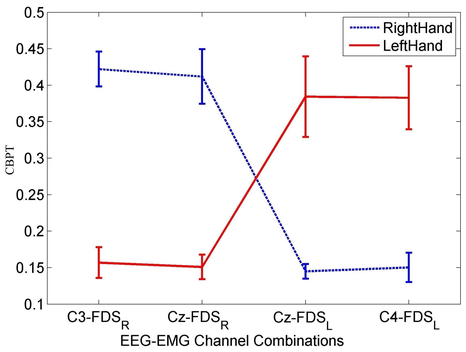


EEG channels: C3, Cz, C4
Left and Right EMG channels: FDS$_L$ and FDS$_R$

Comparison of Classification Accuracy(CA) between CBPT and CMC

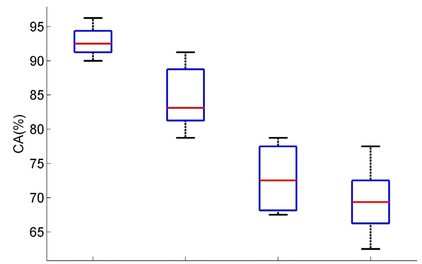


H2: Healthy group who used CBPT based BCI
H1: Healthy group who used CMC based BCI
P: Patient Group

# An EEG-EMG Correlation-based Brain-Computer Interface for Hand Orthosis Supported Neuro-Rehabilitation

Anirban Chowdhury[a,*], Haider Raza[b], Yogesh Kumar Meena[c], Ashish Dutta[a], Girijesh Prasad[d]

[a] *Centre of Mechatronics, Indian Institute of Technology, Kanpur, India*
[b] *School of Computer Science and Electronic Engineering, University of Essex*
[c] *Department of Computer Science, Swansea University*
[d] *School of Computing and Intelligent Systems, Ulster University*

**Abstract**

*Background:* Corticomuscular coupling has been investigated for long, to find out the underlying mechanisms behind cortical drives to produce different motor tasks. Although important in rehabilitation perspective, the use of corticomuscular coupling for driving brain-computer interface (BCI)-based neurorehabilitation is much ignored. This is primarily due to the fact that the EEG-EMG coherence popularly used to compute corticomuscular coupling, fails to produce sufficient accuracy in single-trial based prediction of motor tasks in a BCI system.

*New Method:* In this study, we have introduced a new corticomuscular feature extraction method based on the correlation between band-limited power time-courses (CBPT) associated with EEG and EMG. 16 healthy individuals and 8 hemiplegic patients participated in a BCI-based hand orthosis triggering task, to test the performance of the CBPT method. The healthy population was equally divided into two groups; one experimental group for CBPT-based BCI experiment and another control group for EEG-EMG coherence based BCI experiment.

*Results:* The classification accuracy of the CBPT-based BCI system was found to be $92.81 \pm 2.09\%$ for the healthy experimental group and $84.53 \pm 4.58\%$ for the patients' group.

*Comparison with existing method:* The CBPT method significantly ($p-$value $< 0.05$) outperformed the conventional EEG-EMG coherence method in terms of classification accuracy.

*Conclusions:* The experimental results clearly indicate that the EEG-EMG CBPT is a better alternative as a corticomuscular feature to drive a BCI system. Additionally, it is also feasible to use the proposed method to design BCI-based robotic neurorehabilitation paradigms.

*Keywords:* Corticomuscular-Coherence (CMC), correlation between band-limited power time-courses (CBPT), Electroencephalogram (EEG), Electromyogram (EMG), Hybrid Brain-computer interface (h-BCI), Hand Orthosis, Neurorehabilitation.

## 1. Introduction

The field of bio-robotics has found extensive application in the field of assistive technology and rehabilitation [1]. These include switching or controlling different neuro-prosthetic devices, wheelchairs, and exoskeletons for therapeutic or daily living activities [2]. Some of these rehabilitative settings are based on brain signals such as electroencephalogram (EEG) or magnetoencephalogram (MEG) [3, 4, 5, 6, 7, 8, 9], while some others depend on bio-signals such as electromyogram (EMG) [10, 11]. Using brain or muscle signals alone for the actuation and control of external devices poses their own challenges. The brain signal based controls often suffer from issues such as lower accuracy and need user-specific adaptation for ensuring the reliability [12, 13, 14]. The performances of EMG-based controls are also limited primarily because some of the patients suffering from neuro-muscular diseases may have little or no residual EMG activity, and may suffer from the spasticity and fatigue-related alterations in EMG activity [15]. Therefore, a new shift towards combining different biological signals with the brain signals to enhance its practical usability is becoming popular and many new brain-computer interface (BCI) paradigms are coming up out of this hybridization [16, 17, 18, 19, 20]. Researchers have tried many different ways of fusing EEG and EMG signals to reduce the rate of false positives and enhance the reliability of the BCI system for movement intention detection [21, 22, 23].

Researchers have also stressed that simultaneous activation of cortical and muscular events lead to faster recovery from the motor disability and therefore a correlation between cortical rhythm desynchronization and EMG activation should be an important feature of neurofeedback provided in the rehabilitation process [24, 25]. Importantly, combined EEG-EMG based BCI approaches developed so far, do not make use of the functional communication between EEG and EMG directly as a feature for task classification, rather their associated features are calculated separately and then combined sequentially or simultaneously using a balanced weight or Bayesian fusion approach [1, 26]. A popular method of measuring the cortico-muscular interaction is to calculate the coherence between the EEG and EMG signals, which is called the corticomuscular coherence (CMC). It reveals the mechanism of functional connectivity for the cortical neuron and the motor-unit synchronization [27, 28]. Early works by [29, 30] have shown beta range coherence between MEG/EEG and EMG signals to be significant in voluntary movement and sub-maximal static contraction. Further studies have suggested that CMC is a contralateral phenomenon and it generally gets affected by stroke [31, 32]. CMC is also found to be shifted from beta to gamma range during dynamic force output [33] and different task-specific modulations are found due to the demand of precision or muscle fatigue [34, 35]. Different finger motion classification has also been done using CMC and researchers indicated its possible use for designing multimodal BCI system for the movement intention detection [36, 37, 38]. Although, CMC gives a good estimation of the functional interaction between the brain and muscle after averaging over

*Anirban Chowdhury is a corresponding author

*Email addresses:* anir@iitk.ac.in (Anirban Chowdhury), raza-h@email.ulster.ac.uk (Haider Raza), Meena-Y@email.ulster.ac.uk (Yogesh Kumar Meena), adutta@iitk.ac.in (Ashish Dutta), g.prasad@ulster.ac.uk (Girijesh Prasad)

multiple trials, the single trial based estimation of CMC may not be sufficiently accurate to correctly trigger contingent neurofeedback. CMC needs longer epochs for having good frequency resolution, which is difficult to accommodate in a single-trial based neurofeedback generation as it would include a larger delay in the system [39, 40, 41]. This is primarily due to the inter-trial inconsistency of the CMC caused by the presence of non-stationary changes in the EEG data. One of the major concerns is the reduction in maximum coherence value in case of stroke patients and its dynamic shift in frequency across different time segments [41, 42]. Other pitfalls related to CMC includes lower information content, estimation vs. frequency resolution issues, and lower signal-to-noise ratio (SNR), especially for slow finger motions involving lower muscle mass.

Therefore, we have investigated here a new method of estimating the functional relation between brain and muscle activity which could be used in single trial basis to trigger neurofeedback contingent to the motor execution. This new method termed as CBPT builds on two widely known phenomena associated with the EEG and EMG in relation to motor execution. While attempting a motor task the SMR desynchronization/synchronization occurs in the primary motor cortex, while the EMG activity increases in the corresponding muscle associated with the task. We hypothesized that if we are able to compute the correlation between these changes in the EEG and EMG, we would be able to capture an index of interaction between them. We may look at these two phenomena separately, which could also serve the purpose, but we wanted to deal with corticomuscular relationship angle also, which led us to check the dependency between the two signals in the form of a correlation between them. The developed EEG-EMG interaction index builds on the rationale that for hand rehabilitation it is better to use the relationship between the EEG and EMG signals rather than merely looking at their presence regarding a movement onset. The proposed index not only ensures that a person is engaged with the task both mentally and physically but also gives us an estimate of the quality of this engagement by measuring the relationship between the brain (EEG) and the muscle (EMG) signals. For comparison purpose, we have equipped our BCI system to be operated with both CMC and CBPT features, but one at a time. The current study highlights two aspects of the newly proposed CBPT method. The first is its superiority over the CMC method in terms of the BCI performance. This has been done by comparing two groups of the healthy population, where one group was given CMC-based neurofeedback and another one was given the CBPT-based neurofeedback, in the BCI environment. Second, we have also tested the feasibility of the CBPT-based BCI system on hemiparetic stroke patients for triggering a hand orthosis device. This shows the potential of the CBPT method to be applicable to the BCI-based neurorehabilitation system.

## 2. Materials and Methods

### *2.1. System Overview*

The BCI system developed to test the performance of the corticomuscular features under consideration is equipped with a g.USBamp (g.tec, Graz, Austria) bio-signal amplifier,

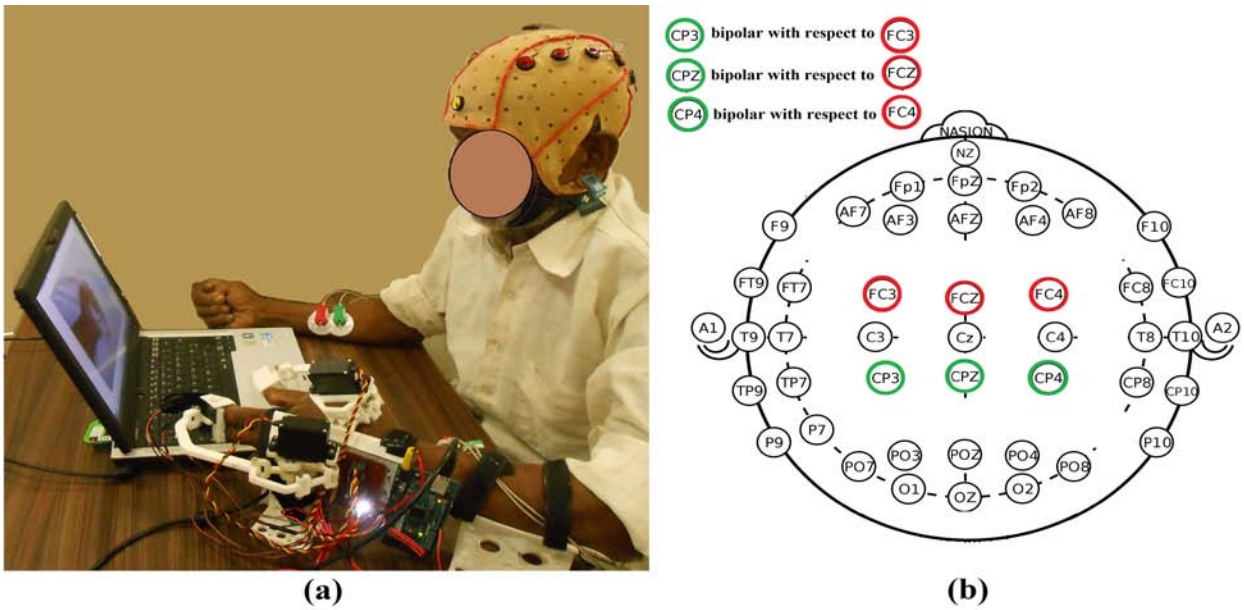


Figure 1: (a) Experimental environment: Participant is triggering the hand orthosis using the BCI paradigm. Electrodes are connected to head cap and forearm muscle to acquire EEG and EMG signals. Neurofeedback is also provided in a visual form in terms of virtual hand grasp, along with proprioceptive feedback using hand orthosis. (b) EEG electrode placement: Electrodes were placed only at the positions which are colored in red/green.

EEG cap (g.tec), Ag/AgCl-based EEG electrodes and sEMG electrodes for the data acquisition. The BCI paradigm, data processing, neurofeedback generation, and database management were designed using a homegrown Graphical-User-Interface (GUI)-based application in MATLAB with Simulink and MS-Access in the backend. The application was run on a Dell Precision 7510 mobile workstation. Neurofeedback was provided in two modes: (*i*) actual finger motion using a hand orthosis and (*ii*) visual feedback of the same motion on the computer monitor. The hand orthosis, developed in-house, is an easy to wear, lightweight, portable device, to support flexion and extension of the index finger, middle finger, and thumb of patients with hand impairment [43]. The index and middle fingers were coupled and driven jointly with a four-bar mechanism. The thumb was driven separately by another four-bar mechanism. Each mechanism was driven by a servomotor having position feedback controller. Hence only two motors need to be actuated for flexion and extension of the three fingers [44]. The BCI was used here only to trigger the orthosis, after which it performs one-time flexion-extension of the users' fingers in a predefined trajectory similar to a normal human finger trajectory. The experimental environment is shown in figure 1(a), while the process flow of the two types of BCI discussed here, is shown in figure 2.

### *2.2. Experimental Protocol*

The experiment was divided into three runs of approximately 7.5 min each with the BCI setup described in Section 2.1. The first two runs were for gathering the training data from which the features were extracted to build a classifier, which was to be used in the

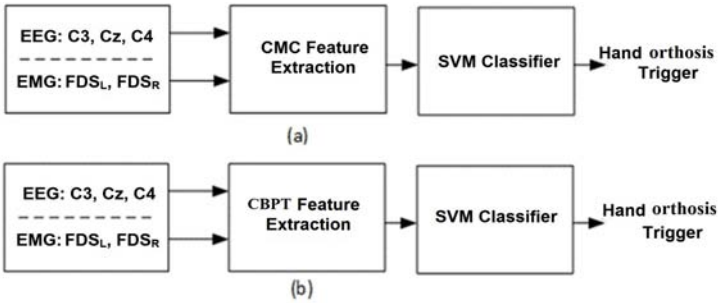


Figure 2: The process flows: (a) CMC-based BCI, (b) CBPT-based BCI.

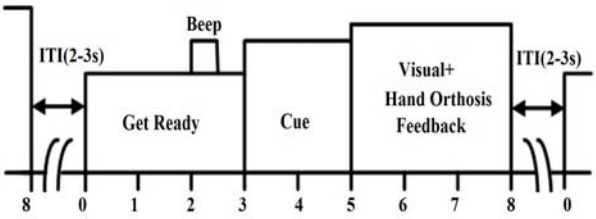


Figure 3: The Timing diagram of the experimental paradigm during neurofeedback stage. Here, grasping motion initiated at 5 s and completed at 8 s, as the orthosis always takes 3 s to complete the grasping motion. If the initiation starts earlier than 5 s i.e. between 3 s to 5 s, then the trial terminates earlier than 8 s.

online feedback generation phase. The third run was to generate neurofeedback on the basis of the trained classifier and thereby its accuracy was tested. All the runs were composed of 40 trials equally divided between two classes of left and right-hand movement and the appearance of the cues was random. Unlike the rest vs. movement paradigm using the one hand only, we incorporated left vs. right-hand paradigm as it has been suggested in an earlier study involving hemiplegic patients [45]. The importance of the orthosis used in this study lies in the fact that we are projecting the CBPT method for building the BCI-based hand rehabilitation therapy, wherein robotic feedback is often suggested for recovery. The current approach of trigged-feedback was used in many previous studies as well, wherein the orthosis was triggered once in a trial upon successful detection of the participants' movement intent [3, 46].

All the trials within a particular run start with a 3 s of preparatory period, during which there was a *GetReady* message on the screen. A beep sound occurred after 2 s within this preparatory stage and lasts for 0.5 s. Then at the end of the preparatory stage, an image of a fisted hand appeared either at the left or right side of the screen. The participants had to make a hand grasp attempt while wearing the orthosis in one of the hands, according to the issued cues. The healthy participants wore the hand orthosis on their right hand and the patients wore the orthosis on their impaired hand. The grasp-attempt was not a full execution but to exert the finger-tip force on the finger-mount caps attached to the orthosis end-effector, so that the EMG signals may be generated in the forearm muscle. Attempted motions are often suggested rather than imagined movements as it is more intuitive and

consequently enhances the BCI performance [47]. In the training phase, the cue lasted for 5 s and in the feedback phase it lasted for 2 s and then the neurofeedback is triggered for 3 s. Thus after elapsing of 5 s after cue, a blank screen appeared in both the training and feedback phases to mark the end of that trials. The gap between the two trials was random between 2 s to 3 s, during which the screen remains blank. Although the appearances of the left and right cues are random, their total appearance in a particular run is equal, i.e. in the run of 40 trials; 20 are left and 20 are right. Therefore it would be a balanced classification problem where the chance level is 50%. Figure 3 shows the timing diagram of the experimental paradigm. The grasping action was initiated by the participants within the 3 s to 5 s period in the trial (i.e. 0 s to 2 s after the cue, as the cue was given at 3 s), and once initiated, the orthosis performs the grasping motion for the fingers and it takes 3 s to complete. For example, if it starts at 5 s(shown in figure 3) then it is completed at 8 s, which is the maximum length of the trial.

### *2.3. Data Acquisition*

The data were recorded from the three EEG and two EMG channels sampled at 512 Hz. The EEG channels were recorded in bipolar mode from $C3$, $Cz$, and $C4$ based on $10-20$ international system electrode positions. The electrodes were actually placed around the specified channel locations (C3, Cz, and C4), keeping the designated area in the middle. The placement of the EEG electrodes on the scalp is shown in figure 1(b) with red/green colored circles. The EEG electrodes were placed at FC3, CP3, FCz, CPz, FC4, CP4 locations according to the 10-20 international system. The channels CP3, CPz, and CP4 were in bipolar with respect to FC3, FCz, and FC4 accordingly. The EMG electrodes were also placed bipolarly on right and left flexor-digitorum-superficialis (FDS) muscle (i.e. $FDS_R$ and $FDS_L$, respectively). Signals were filtered with a pass-band of 0.1 to 100 Hz with a notch filter at 50 Hz to remove power-line artifacts.

### *2.4. Participants*

16 healthy and 8 hemiplegic patients having no prior experience in operating a BCI system participated in the experiments. The patients, who had no history of epilepsy and scored at least 7/10 in Hodgekinsons mini-mental test score, were considered for the experimentation. The participants were sitting in an upright position at approximately 0.5 m to 0.6 m distance from the screen. The demographics of the patients along with their impaired conditions measured in terms of Action Research Arm Test (ARAT) score are shown in Table 1. ARAT measurement, introduced by Lyle et al. [48] is also a reliable way of testing the upper-limb functionality by checking the grasp, grip, pinch and gross-movement activities. The healthy participants were randomly divided into two groups of 8 people, namely H1 and H2. The group distribution was well balanced with group mean age in H1 as 30.5±2.4 years and H2 as 30.87±2.6 years; all of them were male and right-handed. The group H1 performed the CMC-based BCI task and the group H2 performed the CBPT-based BCI task. All the participants gave written consent before the experiment, and all experimental procedures were approved by the institute ethics committee at Indian Institute of Technology, Kanpur.

Table 1: Demographics of the Patient Group (P)

| Variables | Participant ID | | | | | | | |
|---|---|---|---|---|---|---|---|---|
| | **P01** | **P02** | **P03** | **P04** | **P05** | **P06** | **P07** | **P08** |
| **Age** (years) | 59 | 48 | 71 | 35 | 24 | 45 | 62 | 51 |
| **Gender** | M | M | M | F | M | F | F | F |
| **Impaired side** | L | L | L | R | L | L | L | R |
| **Dominant side** | R | R | R | R | R | R | R | R |
| **Time since stroke (months)** | 17 | 8 | 8 | 3 | 8 | 6 | 6 | 48 |
| **ARAT Score** | 32 | 27 | 34 | 7 | 12 | 4 | 40 | 26 |

### *2.5. Feature Extraction and Classification*

After the training runs were over, the acquired EEG and EMG data along with the time-stamps, trigger, and label signals were fed to a data processing algorithm for feature extraction and classification. The algorithm first takes out all the trial segments from the two runs guided by the trigger and label signals, to make the training dataset. Then CMC or CBPT (CMC for H1; and CBPT for H2) feature extraction techniques were applied separately on the training data to train a support vector machine based classifier with a linear kernel. To determine which optimal time segment would be suitable for extracting the CMC/CBPT features, we windowed the 2 s time period after the cue, with a window size of 1 s and a shift of 128 ms. Out of these time windows, the best one having the highest 10-fold cross-validation accuracy was chosen for the neurofeedback generation in the online feedback phase. This has been depicted in figure 4. In the online neurofeedback phase, the 1-s time window between the 0-2 s period after the cue, pre-selected during the training phase, was used for the calculation of the CMC/CBPT features. Suppose, from the analysis of the training dataset, it is seen that the 1-s period between 0.128-1.128 s yielded maximum cross-validation accuracy, then this period was only used for the CMC/CBPT calculation in the online feedback phase. The identification of this 1-s period for CMC feature extraction is subject specific. The CMC- and CBPT-based feature formation process is presented in the following section.

#### *2.5.1.* ***CMC-based feature:***

The functional interaction between two signals $x$ and $y$ in the frequency domain is estimated by the coherence values calculated for the frequencies of interest. The magnitude-squared coherence value between $x$ and $y$ at frequency $f$ can be calculated by the following the standard formulation [49].

$$C_{xy}(f) = \frac{\left|S_{xy}(f)\right|^2}{\left|S_{xx}(f)\right|^2 \times \left|S_{yy}(f)\right|^2} \tag{1}$$

where,

$$S_{xy}(f) = \frac{1}{n}\sum_{i=1}^{n} x_i(f).y_i^*(f) \tag{2}$$

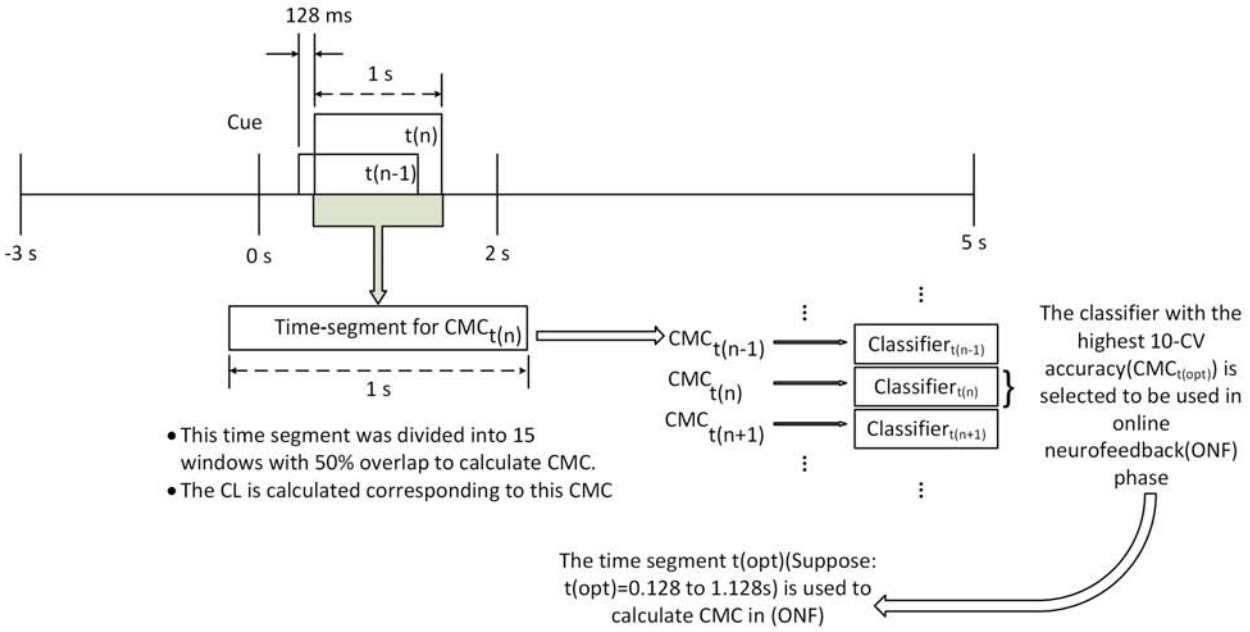


Figure 4: The CMC estimation of a particular trial to show how the windowing for the CMC calculation is different from the windowing of suitable time segment selection for CMC feature extraction.

$$S_{xx}(f) = \frac{1}{n}\sum_{i=1}^{n} x_i(f).x_i^*(f) \tag{3}$$

$$S_{yy}(f) = \frac{1}{n}\sum_{i=1}^{n} y_i(f).y_i^*(f) \tag{4}$$

Here, $S_{xy}(f)$ is the cross-power spectral density of x and y, while $S_{xx}(f)$, $S_{yy}(f)$ are the auto-power-spectral density of $x$ and $y$ respectively. For each of the coherence value calculation, the significance can be checked corresponding to a desired level of confidence $\alpha$ with the following equation [50],

$$CL(\alpha) = 1 - (1-\alpha)^{\frac{1}{n-1}} \tag{5}$$

where $n$ is the number of segments and $CL$ is the level of coherence value to meet the $\alpha$ confidence level. Further, we would like to clarify that while calculating the coherence the data segment was divided into 15 segments, (i.e. $n = 15$). This means that the 1 s period, which was used for the coherence calculation, was divided into windows of 125 ms with 62.5 ms shift i.e. the overlap between the two consecutive windows was 50%. The confidence limit can be changed by changing the number of segments the data is divided into, which is $n$. We have experimentally set the number $n$ for coherence calculation to 15, by considering spectral smoothing aspect for keeping the confidence limit as low as possible. It is true that if we increase the value of $n$ (i.e. increasing the number of segments and

reducing the window size) the coherence spectrum would be smoothed and the $CL$ would go down; but at the same time, the magnitude of the peak coherence will also go down. The reverse is also true; that is if we keep $n$ small, then $CL$ and the peak coherence magnitude will also go higher and the coherence spectrum would be jittery. Hence, there should be a trade-off for choosing the value of $n$ so that the coherence spectrum could be smooth enough and $CL$ is lower enough as compared to the peak coherence magnitude. After doing several trials with the value of $n$ we kept it at 15, in order to get an optimal performance. It is to be noted that we haven't done any sum of coherence estimates across frequency ranges but only the maximum coherence value above the chance level over the spectrum of 15-40 Hz (i.e. Beta and Gamma range) was considered as the CMC features.

Thus the coherence between one channel of EEG and one channel of EMG can be calculated for the frequency $f$ from their cross and auto power spectral density using equation (1)-(4). The EMG signal was rectified before CMC calculation. To form the feature vector, we considered only the contralateral and midline coherence values between EEG and EMG within beta ($\beta$) and gamma ($\gamma$) frequencies. In a particular trial, the coherence spectrum between 15 Hz to 40 Hz for the channel combinations $C3-FDS_R$, $Cz-FDS_R$, $Cz-FDS_L$ and $C4-FDS_L$ were first obtained. The maximum coherence value over the coherence spectrum from all the four different channel combinations was grouped together to form a feature vector of four elements corresponding to that particular trial. Thus an $80 \times 4$ feature space was generated from two training runs where each of the classes had $40 \times 4$ feature space. These features were then used to train a support vector machine (SVM) classifier. Here we have considered only those values of coherence which met the 95% confidence level criterion. As we have taken $n = 15$ during coherence calculation, therefore according to equation (5), any coherence value less than 0.19 is considered insignificant and is replaced by zero during feature generation.

#### *2.5.2.* ***CBPT-based feature***

In this method, we have used the correlation between the band-limited power time-courses associated with EEG and EMG signals to measure the functional interaction between brain and muscle. The calculation of the CBPT index is described as follows.

Suppose we have raw EEG data and EMG data from $i^{th}$ trial, which are denoted as $rEEG_i$ and $rEMG_i$, respectively. As CBPT focuses on correlating the change in EEG and EMG band-power, therefore, a key thing is to find desired frequency bands where this change occurs simultaneously. It is widely known that Sensorimotor Rhythm (SMR) desynchronization happens both in mu ($8-12$ Hz) as well as beta ($16-24$ Hz) bands related to the motor execution/imagery [4]. Recently, the importance of beta band is also stressed upon relating to the stroke rehabilitation [51]. Hence, we needed to look at both mu and beta ERD to determine which SMR desynchronization would be more suitable for CBPT. We have compared the mu and beta ERD based on their distribution over the trials and chosen the frequency band which has less inter-trial variability, irrespective of the median value of the distribution. From the figure 5 we can see that although the median of beta ERD is more than the mu ERD, the distribution of mu ERD is more compact than the beta ERD, meaning that the inter-trial variability is less in case of mu. Therefore, we have

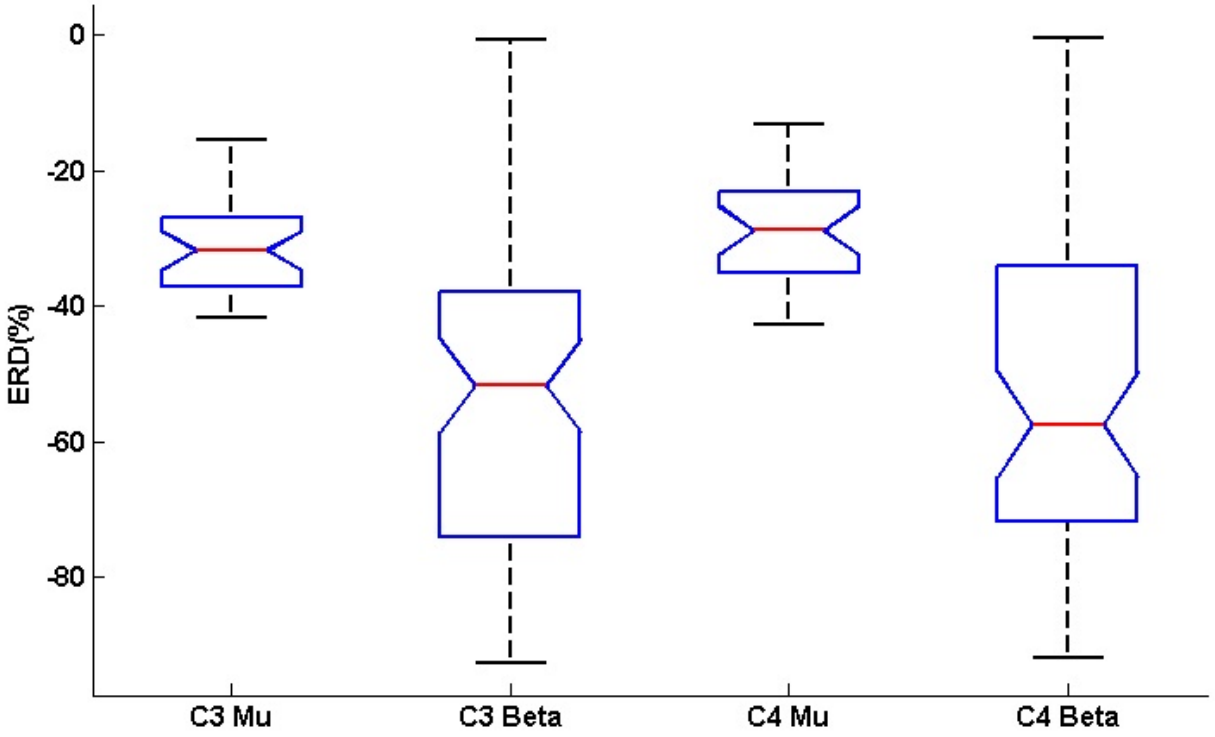


Figure 5: The ERD distribution of the mu and beta bands to show the contralateral activation during the motor task. The distribution of C3 Mu and C3 Beta is during right-hand task and C4 Mu and C4 Beta is during left-hand task. The distribution is plotted over healthy group H2 (who used the CBPT based BCI) for all the calibration stage trials. It can be seen that although the median of the ERD for Beta band is almost twice as that of Mu, the distribution of Mu ERD is more compact over the trials (i.e. the inter-trial variability is less.)

chosen the mu band for the calculation of CBPT. The change in EMG power occurs in a larger frequency spectrum, 5 to 150 Hz, with a peak in between $50-60$ Hz. But the SNR is comparatively low for the signal below 15 Hz. Therefore, we have taken the EMG frequency band between 30 Hz and 50 Hz, i.e. the rising edge of the power spectrum [52]. Thus, the EEG and EMG signals were band-pass-filtered in their desired frequency bands, e.g. mu ($\mu$) band $[8-12]$ Hz for the EEG signal and $[30-50]$ Hz for the EMG signal. After the band-pass filtering, we denote EEG and EMG signals as $bEEG_i$ and $bEMG_i$, respectively. Then $bEEG_i$ and $bEMG_i$ are squared to get the band-power $pEEG_i$ and $pEMG_i$ respectively. The $pEEG_i$ and $pEMG_i$ are then smoothed using a moving window average (window size 1 s for EEG and 30 ms for EMG) to get $smEEG_i$ and $smEMG_i$, respectively. This smoothing step is necessary to get the gradual change in the EEG and EMG data. Without smoothing the fluctuations in the signal would be high, resulting into lower correlation coefficients. The smoothing time window was selected empirically for the EEG and EMG signals to increase the feature separation between the two classes. Finally the correlation between $smEEG_i$ and $smEMG_i$ is calculated over a suitable time period of 1 s which falls between 3 s and

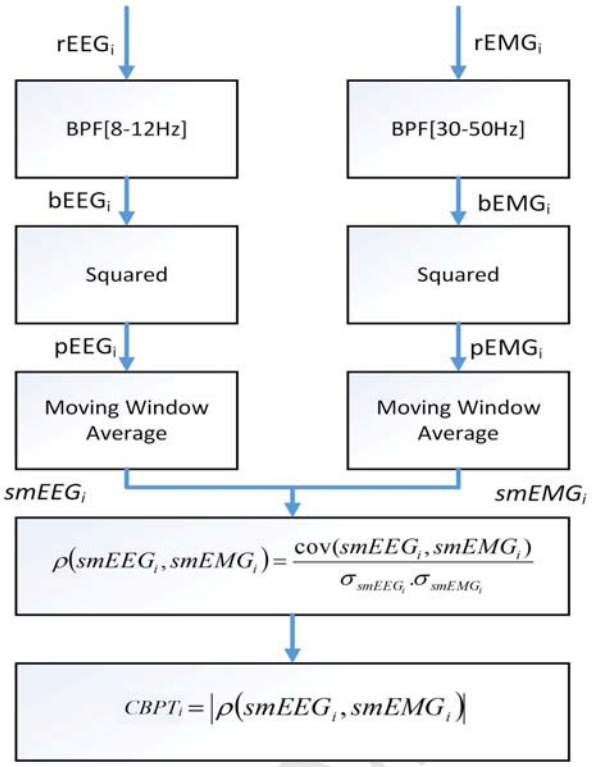


Figure 6: Process flow of the CBPT feature calculation.

5 s within a trial, where 3 s is the instant of cue appearance. The correlation is given by the equation (6).

$$\rho(smEEG_i, smEMG_i) = \frac{cov(smEEG_i, smEMG_i)}{\sigma_{smEEG_i}.\sigma_{smEMG_i}} \tag{6}$$

where, $\rho(smEEG_i, smEMG_i)$ is the correlation coefficient between $smEEG_i$ and $smEMG_i$; cov($smEEG_i$,$smEMG_i$) is covariance between $smEEG_i$ and $smEMG_i$; and $\sigma(smEEG_i)$ and $\sigma(smEMG_i)$ are the standard deviation of $smEEG_i$ and $smEMG_i$ respectively. Thus $CBPT_i$ denoted by $\left|\rho(smEEG_i, smEMG_i)\right|$ is the band-power correlation index at the $i^{th}$ trial between one specific channel of EEG and another specific channel of EMG. In our study, we have calculated this index for the same combination as in the case of CMC (i.e. $C3 - FDS_R$, $Cz - FDS_R$, $Cz - FDS_L$, and $C4 - FDS_L$) to make a feature vector of four elements. This process is depicted in a block diagram in figure 6. It is to be noted that the correlation values below an arbitrary threshold were set to 0, so as to avoid the effect of misleading correlations. Our current investigation focuses on finding out the discrimination between the two classes based on the developed EEG-EMG interaction index, which is also found to be varying between the patient and the healthy participants, bearing the evidence that the impaired corticomuscular interaction can be reflected by the developed EEG-EMG

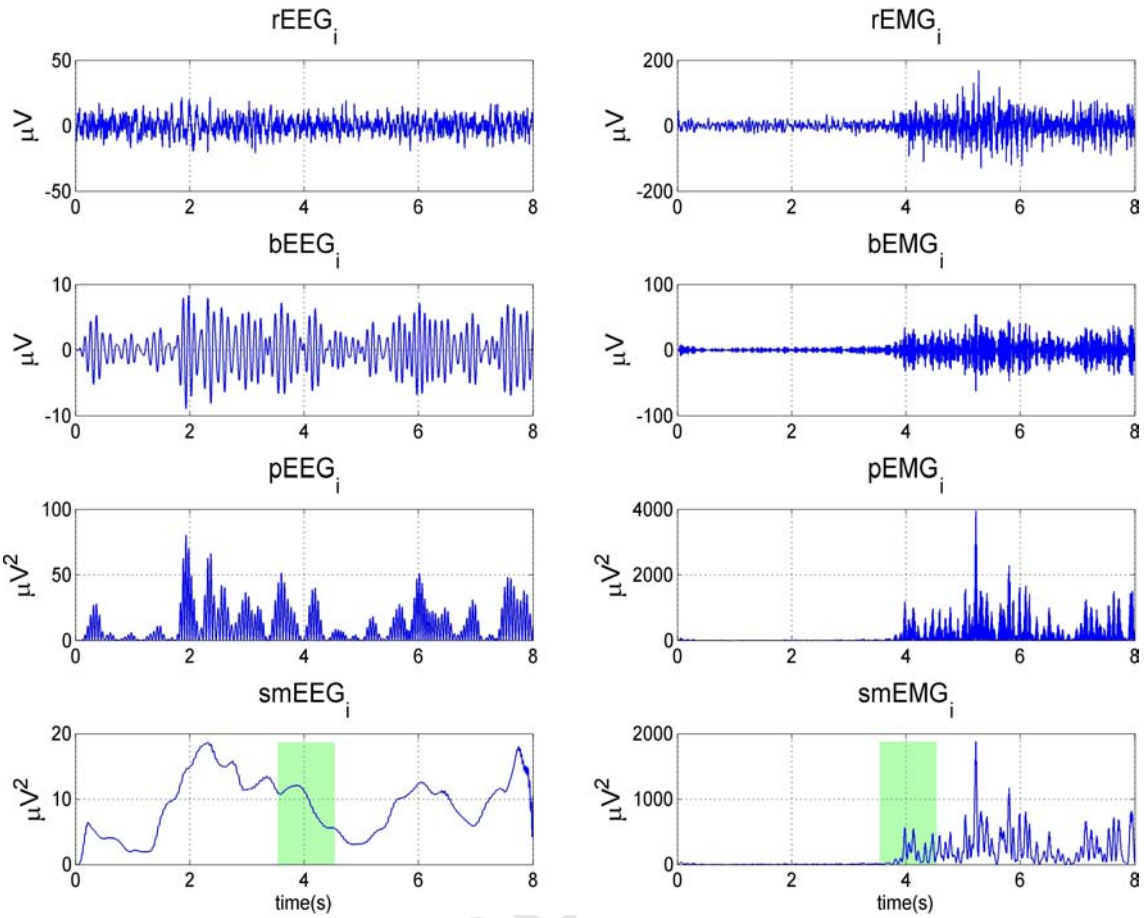


Figure 7: The process of EEG and EMG signal transformation in a single-trial, for the calculation of CBPT index, is shown in two-panel row-wise. An example is taken from the 1st trial of participant P01 of group H2 during 1st run of the training session. The Left panel is showing the transformations of the EEG signal and the right panel is showing the transformations of EMG signals. The correlation is calculated between the EEG and EMG signal portion shaded with green color in the bottom row of the figure.

interaction index.

In the example shown in figure 7, we have taken the data of one particular trial from the participant P01 of group H2 and shown how to process the EEG and EMG signals, step-by-step, to reach up to smoothened power variation from the raw signals. We then selected a suitable time window, the same for both EEG and EMG signals, and calculated the correlation coefficient between them. In this example, 0 s to 8 s is the entire trial period in which the cue appeared at 3 s. We have taken a time span of 3.536 s to 4.536 s to calculate the correlation, whose absolute value is the CBPT index. It is to be noted that the best time span of feature extraction has been calculated for each participant separately, (the time span having the highest 10-fold cross-validation accuracy on the training data is selected for a particular participant, which was kept fixed in the feedback phase); hence it is not fixed for all participants.

*2.5.3. Advantage of CBPT over CMC*

In order to illustrate why CBPT is a novel methodological advancement over the conventional CMC, we highlight next the importance of CBPT in finding the relation between EEG and EMG when the changes corresponding to a single corticomuscular phenomenon is occurring in two different frequency bands in the two different signals (EEG and EMG), whereas CMC looks for the interaction between the EEG and the EMG at the same frequency. This is also evident from the power spectral density (PSD) of the EEG and the EMG signals as they differ quite a bit. For example, the EEG signal modulations regarding the motor actions are confined in 8-30 Hz, while the corresponding changes in the EMG may happen beyond 30 Hz as EMG has a much wider spectrum. In the following example, we would see how the CBPT can handle such situations.

Again suppose, there are two signals $x$ and $y$. The signal $x$ has the components 13 Hz, 10 Hz, and 31 Hz, while $y$ has the components 18 Hz, 26 Hz, and 39 Hz. We have modulated the 10 Hz component in $x$ such that its amplitude starts decreasing after 1 s and simultaneously there is an increase in the signal amplitude of the 26 Hz component of the signal $y$. The pictorial representation of the signals $x$ and $y$ along with their components are shown in the figure 8. Now, there is no common frequency where the changes in the $x$ and $y$ are occurring, rather the modulations are on the different frequencies. From the coherence plot of the $x$ and $y$ as shown in figure 9, we see that the information indicating the relationship between $x$ and $y$ is ambiguous here. Moreover, the coherence spectrum is below the confidence limit (0.19).

Next, we use the CBPT technique to capture the modulation relation between $x$ and $y$, following a similar process as given in the Section 2.5.2. The signal $x$ is band-passed over 9-11 Hz, while the signal $y$ is band pass filtered over 25-27 Hz. Then the corresponding band powers in those frequency bands were smoothened with an arbitrary window of 1 s and 30 ms respectively. The transformations of the signals between 1 s to 2 s period (where the modulation happened) after the application of band-power smoothing are shown in figure 10. Now, if we calculate the Pearson's correlation coefficient between the transformed signals of $x$ and $y$, that would yield -0.7083 ($p-$value$<0.05$).

Thus the correlation co-efficient resulting from the CBPT computation facilitates the measurement of interaction between the two signals, where the changes are occurring at same/different frequencies, unlike the CMC which measures the interaction only at the same frequency. In the next section (Section 3), the BCI accuracy results of the single trial based CBPT, as compared to CMC for the same motor task, are presented to show how CBPT overcomes the lower-performance of CMC in generating contingent neurofeedback, which is an essential criterion for corticomuscular feature driven BCI for neurorehabilitation. These two advantages clearly establish the rationale behind engineering a new corticomuscular feature (CBPT), which builds on the limitations of CMC as discussed above.

## 3. Results

We describe the results obtained from each experimental group regarding the feature distribution and classification accuracy. The classification accuracies are compared between

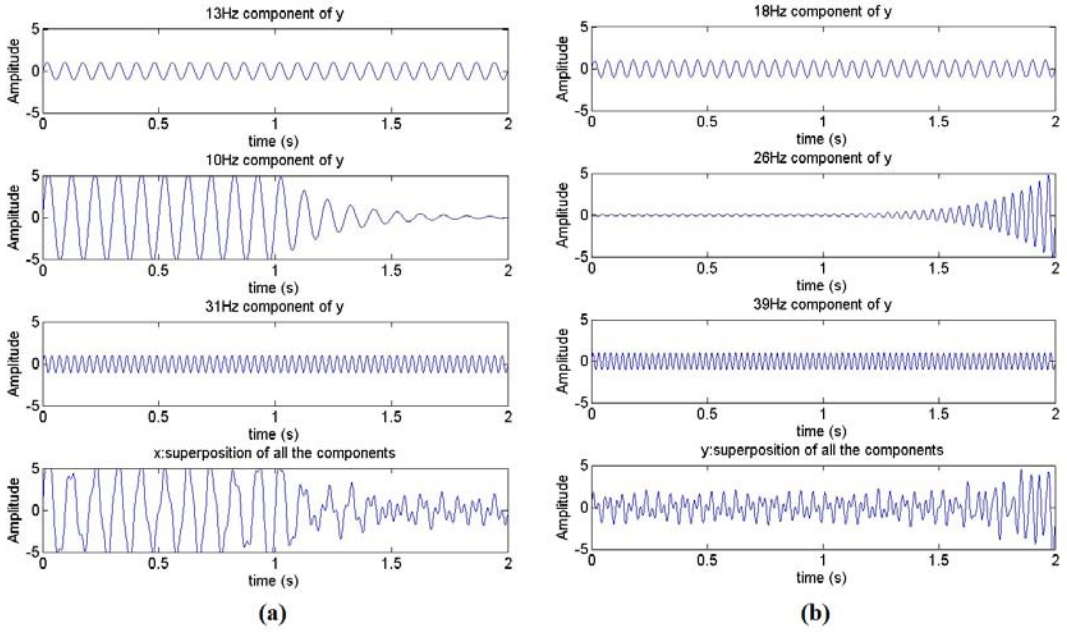


Figure 8: The signals $x$ and $y$. The components of $x$ along with their superposition are shown in (a); the same of $y$ is shown in (b). Both the components 10 Hz and 26 Hz in $x$ and $y$ respectively are modulated so that the amplitude of the former decreases and the amplitude of the later increases after 1 s.

the CBPT-based method and CMC-based method for the healthy participants. Then the performance of CBPT-based BCI on the patient population is described.

In figure 11, we have shown the average CMC feature distribution of all the participants within group H1 for the left and right-hand tasks. The average CMC feature for a particular participant is calculated by taking the average of all the features calculated during the BCI task execution, and further averaged over all the participants. As the features are composed of the maximum coherence values of the $C3-FDS_R$, $Cz-FDS_R$, $Cz-FDS_L$, and $C4-FDS_L$ channel combinations, the average feature is actually the average of all these maximum values across all the trials.

From the average CMC features distribution of healthy group H1 (figure 11), it can be seen that the maximum value of $0.36\pm0.02$ occurred in the case of $C3-FDS_R$, during right-hand task, and the values for other channel combinations were $0.33\pm0.02$ for $Cz-FDS_R$, $0.3\pm0.01$ for $Cz-FDS_L$, and $0.31\pm0.02$ for $C4-FDS_L$. During Left-hand task (figure 11), the average CMC features were $0.27\pm0.01$ for $C3-FDS_R$, $0.27\pm0.01$ for $Cz-FDS_R$, $0.34\pm0.02$ for $Cz-FDS_L$, and $0.35\pm0.02$ for $C4-FDS_L$. It is quite evident from these CMC average feature distributions that for H1 group $C3-FDS_R$ and $Cz-FDS_R$ coherence in right-hand task are clearly higher than those in left-hand task. Also, we notice that the $Cz-FDS_L$ and $C4-FDS_L$ coherence are clearly higher during left-hand task than those in right-hand task for healthy participants of group H1. Next, the CBPT features are shown in figures 12-13. CBPT features are basically the absolute values of correlation calculated for the same channel combination as in the case of CMC (i.e. $C3-FDS_R$, $Cz-FDS_R$,

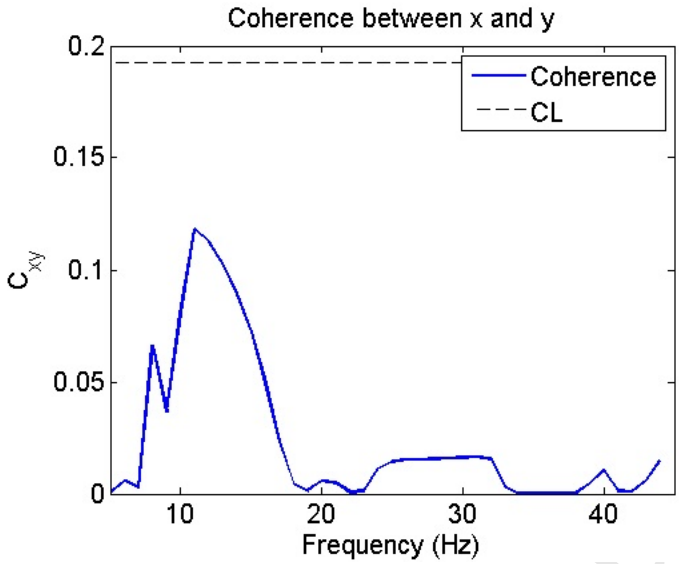


Figure 9: The coherence spectrum for the $x$ and $y$ signals. There is no distinctive feature in the coherence spectrum which can capture the modulation relationship between $x$ and $y$, although it is there and also the coherence spectrum is below the confidence limit ($CL = 0.19$).

Table 2: The average CMC and CBPT feature values

| | **CMC features(H1)** | | **CBPT features(H2)** | | **CBPT features(P)** | |
|---|---|---|---|---|---|---|
| | **Right Hand** | **Left Hand** | **Right Hand** | **Left Hand** | **Right Hand** | **Left Hand** |
| $C3FDS_R$ | $0.36 \pm 0.02$ | $0.27 \pm 0.01$ | $0.41 \pm 0.03$ | $0.14 \pm 0.01$ | $0.21 \pm 0.03$ | $0.16 \pm 0.03$ |
| $CzFDS_R$ | $0.33 \pm 0.02$ | $0.27 \pm 0.01$ | $0.40 \pm 0.03$ | $0.13 \pm 0.02$ | $0.22 \pm 0.02$ | $0.14 \pm 0.03$ |
| $CzFDS_L$ | $0.30 \pm 0.01$ | $0.34 \pm 0.02$ | $0.13 \pm 0.02$ | $0.39 \pm 0.06$ | $0.15 \pm 0.03$ | $0.18 \pm 0.04$ |
| $C4FDS_L$ | $0.31 \pm 0.02$ | $0.35 \pm 0.02$ | $0.13 \pm 0.02$ | $0.39 \pm 0.06$ | $0.14 \pm 0.03$ | $0.19 \pm 0.03$ |

$Cz - FDS_L$ and $C4 - FDS_L$). In order to get this distribution, we calculated the average CBPT feature for each participant in a particular participant group by taking the average of CBPT features across all the trials during the BCI task execution. Figure 12 shows this distribution for healthy participants of group H2 wherein the CBPT values of $C3 - FDS_R$, $Cz - FDS_R$ ,$Cz - FDS_L$, and $C4 - FDS_L$ are $0.41 \pm 0.03$, $0.40 \pm 0.03$, $0.13 \pm 0.02$, and $0.13 \pm 0.02$, respectively during right-hand task and $0.14 \pm 0.01$, $0.13 \pm 0.02$, $0.39 \pm 0.06$, and $0.39 \pm 0.05$, respectively for left-hand task. The same feature distribution in the patient group P can be found in figure 13 for $C3-FDS_R$, $Cz-FDS_R$ ,$Cz-FDS_L$, and $C4-FDS_L$ as $0.21 \pm 0.03$, $0.22 \pm 0.02$, $0.15 \pm 0.03$, and $0.14 \pm 0.03$ respectively during right-hand task and for left-hand task they are $0.16 \pm 0.03$, $0.14 \pm 0.03$, $0.18 \pm 0.04$, and $0.19 \pm 0.03$ respectively. From the distribution it can be seen clearly that $C3 - FDS_R$ and $Cz - FDS_R$ CBPT values are higher in right-hand task than that in left-hand task while $Cz - FDS_R$ and $Cz - FDS_L$ CBPT values have reverse nature in healthy group H2. Similar discrimination between the left and right-hand task is also evident for the patient group $P$ from figure 13 although the gap is not as wide as H2. The CMC and CBPT feature values are shown in Table 2.

The performances of the classifiers using CMC- and CBPT-based features are also plotted for healthy groups H1 and H2 and patient group P in figure 14 in terms of classification

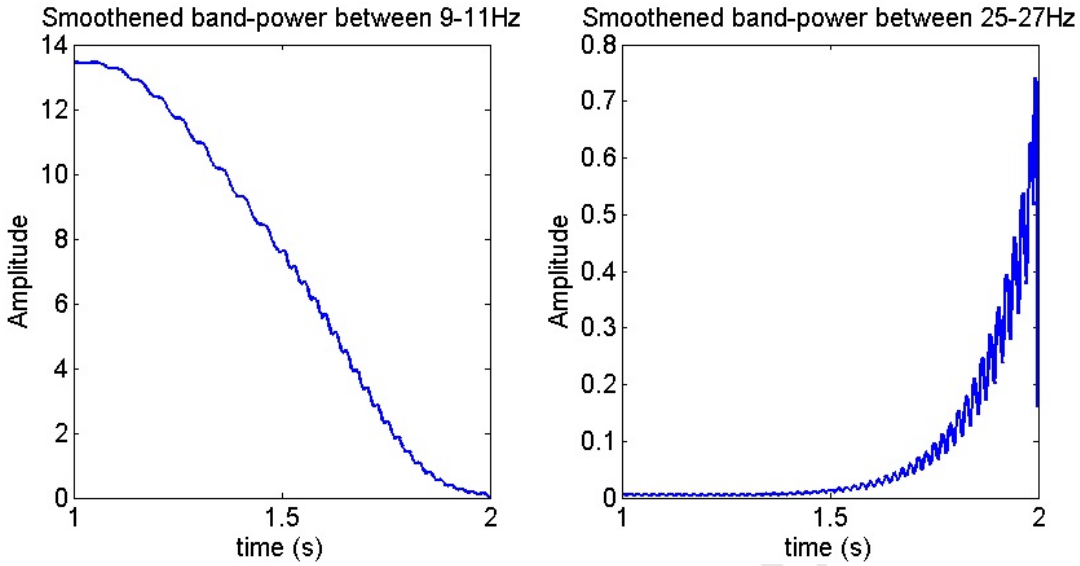


Figure 10: The smoothened band power signals of (a)$x$(band pass filtered over 9-11 Hz and smoothing window 1 s) and (b)$y$ (band pass filtered over 25-27 Hz and smoothing window 30 ms) between 1 s to 2 s. We can see that the modulation trend is vivid in the case of $x$, where it is decreasing and in the case of $y$, where it is increasing. The Pearson's correlation coefficient between these two variations of $x$ and $y$ is -0.7083 with $p-$value$<0.05$.

Table 3: Classification accuracies of different experimental methods applied on different participant groups

| Variables | CBPT H2 | | CBPT P | | CMC H1 | | CMC P | |
|---|---|---|---|---|---|---|---|---|
| | CA (%) | TPs | CA (%) | TPs | CA (%) | TPs | CA (%) | TPs |
| **P01** | 96.25 | 4.536 | 78.75 | 4.536 | 68.75 | 4.792 | 62.55 | 4.664 |
| **P02** | 91.25 | 4.536 | 90.00 | 4.664 | 67.50 | 4.664 | 70.00 | 4.280 |
| **P03** | 92.50 | 4.408 | 91.25 | 4.664 | 78.75 | 4.280 | 72.50 | 4.280 |
| **P04** | 95.00 | 4.536 | 82.50 | 4.408 | 75.00 | 4.408 | 68.75 | 4.664 |
| **P05** | 93.75 | 4.792 | 87.50 | 4.408 | 76.25 | 4.408 | 65.00 | 4.536 |
| **P06** | 91.25 | 4.536 | 83.75 | 4.536 | 78.75 | 4.664 | 72.50 | 4.536 |
| **P07** | 92.50 | 4.536 | 80.00 | 4.280 | 67.50 | 4.280 | 67.50 | 4.792 |
| **P08** | 90.00 | 4.408 | 82.50 | 4.792 | 70.00 | 4.664 | 77.50 | 4.664 |
| Mean | 92.81 | 4.536 | 84.53 | 4.568 | 72.81 | 4.520 | 69.53 | 4.552 |
| Std | 2.09 | 0.119 | 4.58 | 0.190 | 4.90 | 0.199 | 4.72 | 0.187 |

TPs: Time points

accuracy. It is to be noted that the CMC analysis for the patient group was done offline just to confirm the superiority of the CBPT method over the CMC method for achieving higher classification accuracy. The detail of classification accuracy for each group and for each classification method is given in Table 2. The results show the average classification accuracy of H1 for CMC method is $72.81 \pm 4.90\%$, while the classification accuracy of H2 for the CBPT-based method is $92.81 \pm 2.09\%$. A two-tailed paired t-test shows that CBPT-based classifiers have provided significantly ($p < 0.05$) higher accuracy than the CMC-based classifiers for the healthy participants. The time points from which the CMC and CBPT features were calculated are also shown beside every CA values, which show that the average time points for all the groups were above 4.5s. As mentioned in section 2.5 that 1 s time

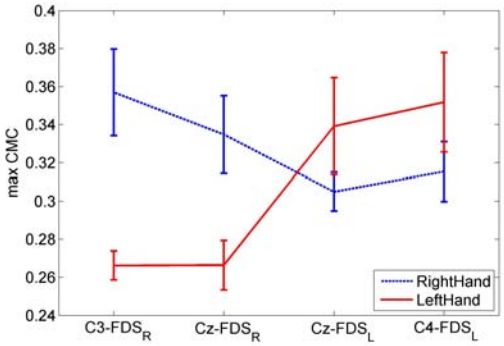


Figure 11: Average CMC feature distribution of healthy participant group H1 for different channel combinations. The vertical bars are depicting the standard deviation of the average CMC value across all the participants.

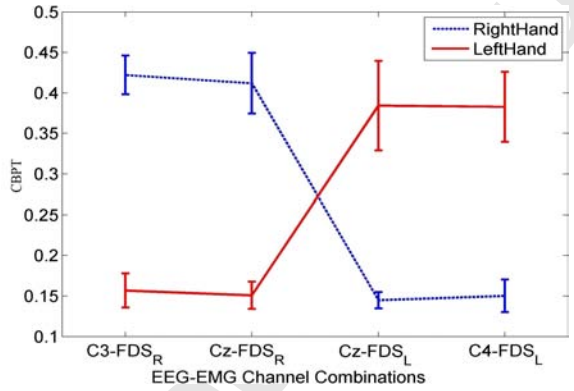


Figure 12: Average CBPT feature distribution of Healthy participant group H2 for different channel combinations. The vertical bars are depicting the standard deviation of the average CBPT value across all the participants.

history before the time point, was used for feature extraction, which means the starting point of the feature extraction time window was approximately after 3.5s. Therefore, the possible effect of the signal portion before the cue appearance, which may arise during the smoothing step of the CBPT feature extraction was mostly avoided. The data from patient group P were also analyzed offline using the CMC method. The offline analysis of CMC on group P resulted in average CA of $69.53 \pm 4.72\%$, which was also significantly ($p < 0.05$) less than the average CA using CBPT on the same group, which was $84.53 \pm 4.58\%$. It is worth mentioning that the comparison between healthy and patient participant populations for the same classification method yielded higher accuracy in healthy groups than in patients.

## 4. Discussion

In the current scope of work, our objective is to find out a suitable neuromarker of corticomuscular functional interaction which can be used as an alternative feature to design a BCI-based neurorehabilitation paradigm. The main motivation is to take into account

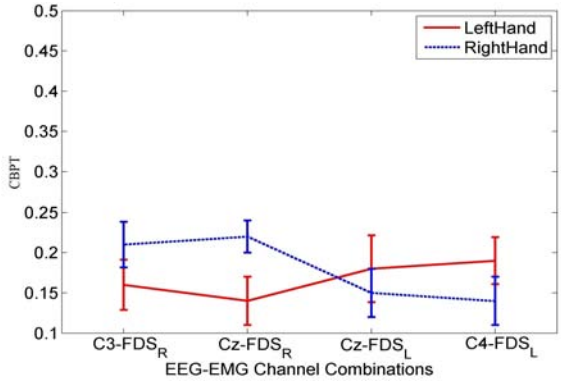


Figure 13: Average CBPT feature distribution of Patient group P for different channel combinations. The vertical bars are depicting the standard deviation of the average CBPT value across all the participants.

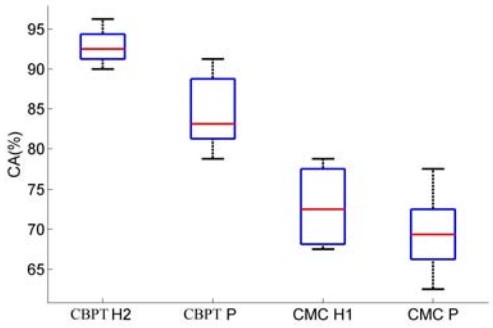


Figure 14: The comparison of classification accuracies among different participant groups undergoing different experimental methods. The top and bottom of each box represent the $25^{th}$ and $75^{th}$ percentiles respectively. The horizontal red line represents the median and the whiskers are drawn from the ends of the interquartile ranges to the minimum and maximum values.

the corticomuscular interaction rather than the usual approach of considering separately computed cortical and/or muscle activity based features. The issue of integrating EEG and EMG in an optimal manner is very critical and studies on this matter often lack clinical validation [1]. Although there are several examples of combining EEG and EMG features in the hybrid BCI literature, they only feed separately calculated EEG and EMG features to a classifier in a simultaneous or sequential manner for decision making. In contrast to that in our work, EEG and EMG signals are considered together, to come up with a unique feature that depicts the interaction between the two. So there is no fusion of features at the classification stage, rather it is done in the feature extraction stage. The CBPT overcomes the limitation of CMC based approach, which fails to achieve sufficient accuracy in single-trial based classification of motor tasks. It is also a shift in conventional paradigm of the BCI, which are not based on corticomuscular interaction, although it is important in rehabilitation perspective. It has also the potential to promote both mental and physical engagement of patients with the task, essential for an effective motor-recovery. The two

possible ways of generating such features are discussed in this paper. The results obtained from the experiments indicate the superiority of the CBPT-based method over the conventional CMC-based method. The performance of CBPT method is found satisfactory for both healthy and patient groups, for use as a possible mode to drive a BCI-based neurofeedback. Additionally, a careful observation of the results presented in the study, reveals that the proposed index has comparatively lower values for the patients than that for healthy individuals (see figure 12-13). This clearly shows that the index is able to capture the quality of interaction between EEG and EMG signals, as the corticomuscular interaction generally gets compromised due to stroke. Hence, we argue that the CBPT index is presented here as a measure of corticomuscular interaction.

CBPT could also be advantageous because of the fact that the magnitude of EMG activity is not important, rather the change in the activity during a task execution is crucial for capturing the correlation between EEG and EMG. The choice of CMC is motivated by the fact that it is associated with descending drives which modulate muscular activity before the movement onset [37, 53]. Moreover, the dependence on EMG only is not as reliable as the stroke patients often suffer from the muscle spasticity resulting in involuntary EMG activation [31]. The EEG-EMG coherence has already shown its potential to be used as an indirect measure of motor recovery which is often linked with neuroplasticity; the neuronal reorganization after stroke [54, 55]. Therefore, further research can be carried out to find out similar measures in terms of CBPT.

As most of the stroke patients in the current study are impaired in left hand (6 out of 8 patients), the features are not so separable for right motor cortex-left forearm muscle ($C4 - FDS_L$) which is shown in figure 13, where the CBPT feature distribution of the patient group is shown. In the case of patients, the distinction between the two classes for CBPT features are not as high as the healthy group. The dominant CBPT features during a particular task in healthy participants are always greater than the dominant CBPT features of patients during that task. Thus it is indicative that the newly proposed CBPT feature is very closely related to the CMC and hence may be a plausible candidate to inquire about corticomuscular interaction. Moreover, in terms of feature separability, CBPT has a clear advantage over CMC, which is further proven by the classification accuracies calculated on the basis of these two features.

The classification accuracy comparisons as shown in figure 14 brings out the fact that the CBPT-based classification has resulted in significantly ($p < 0.05$) higher accuracy than the CMC-based classification for both the healthy and patient groups. Also, we find that for the same method, the classification accuracy of healthy participants is comparatively greater than that for patients. The lower performance rate of the patients may have occurred primarily due to the reduced corticomuscular-connectivity resulting from stroke. Also the other factors like mood and fatigue, both physical and mental, could contribute to lower accuracy as the patients are often found to experience a much higher level of fatigue after stroke.

Although the feasibility of CBPT feature to be used in BCI-based neurorehabilitation system is established here, the motor functional recovery of the stroke patients resulting from its usage can be explored in further studies. The significance of CBPT and CMC as

an indirect outcome measure of recovery can also be explored. Importantly, the variability of CBPT-based BCI performance with fatigue is yet to be tested, as there are many studies on CMC suggesting the fact that the corticomuscular interaction is greatly affected due to fatigue [35, 40]. The patient performance using CBPT and CMC may be further improved by making the BCI paradigm more interesting for the participants, using virtual reality platforms. As the current BCI-based on CBPT needs residual muscle activity and may not be feasible with patients in a flaccid stage, the motor-imagery BCI-based on only EEG signals can be clubbed together with the current paradigm to make a multi-modal or hybrid BCI to cater for all the phases of stroke recovery.

## 5. Conclusion

This paper introduced the correlation between band-limited power time-courses (CBPT) associated with EEG and EMG signals, as a feature to trigger a BCI operated hand orthosis-based neurorehabilitation system. This is a novel technique in line with combined EEG-EMG-based BCI approaches. It outperformed the traditional corticomuscular-coherence-based BCI classification, as the test results in healthy and patients groups have amply demonstrated. Therefore, it can be concluded that the CBPT-based classification could be a highly efficient alternative for designing BCI-based neurorehabilitation system powered by corticomuscular-interaction.

## Acknowledgment

This work was supported in part by the Department of Science and Technology (DST), India and in part by the UK India Education and Research Initiative (UKIERI) Thematic Partnership project "A BCI operated hand Exoskeleton-based neurorehabilitation system" under grant DST/INT/UK/P-80/2014, UKIERI-DST-2013-14/126 and DST-UKIERI-2016-17-0128. The experimentation on patient groups was conducted in collaboration with the Regency Hospital, Kanpur.

## Research Ethics

All procedures performed were in accordance with the ethical standards of the Ethics Committee of the Indian Institute of Technology, Kanpur, India and with the 1964 Helsinki declaration and its later amendments or comparable ethical standards. Informed consent was obtained from all participants included in the study.

## Declaration of interest

The authors declare that we do not have any commercial or associative interest that represents a conflict of interest in connection with the work submitted.

## Author's contributions

GP and AD conceived the study. AC, HR, and YKM designed the experimental setup and analysed the results. AC and YKM collected data. AC, HR, and YKM wrote up the manuscript. GP and AD received funding for the study, advised on study design and reviewed the outcomes. All authors reviewed and approved the final manuscript.

## References


[1] T. D. Lalitharatne, K. Teramoto, Y. Hayashi, K. Kiguchi, Towards hybrid EEG-EMG-based control approaches to be used in bio-robotics applications: Current status, challenges and future directions, Journal of Behavioral Robotics 4 (2) (2013) 147–154. doi:https://doi.org/10.2478/pjbr-2013-0009.

[2] G. Müller-Putz, R. Leeb, M. Tangermann, J. Höhne, A. Kübler, F. Cincotti, D. Mattia, R. Rupp, K.-R. Mueller, J. D. R. Millán, Towards noninvasive hybrid brain–computer interfaces: framework, practice, clinical application, and beyond, Proceedings of the IEEE 103 (6) (2015) 926–943. doi:https://doi.org/10.1109/JPROC.2015.2411333.

[3] E. Buch, C. Weber, L. G. Cohen, C. Braun, M. A. Dimyan, T. Ard, J. Mellinger, A. Caria, S. Soekadar, A. Fourkas, et al., Think to move: a neuromagnetic brain-computer interface (bci) system for chronic stroke, Stroke 39 (3) (2008) 910–917. doi:https://doi.org/10.1161/STROKEAHA.107.505313.

[4] G. Prasad, P. Herman, D. Coyle, S. McDonough, J. Crosbie, Applying a brain-computer interface to support motor imagery practice in people with stroke for upper limb recovery: a feasibility study, Journal of NeuroEngineering and Rehabilitation 7 (1) (2010) 60. doi:https://doi.org/10.1186/1743-0003-7-60.

[5] J. d. R. Millán, R. Rupp, G. R. Müller-Putz, R. Murray-Smith, C. Giugliemma, M. Tangermann, C. Vidaurre, F. Cincotti, A. Kübler, R. Leeb, et al., Combining brain–computer interfaces and assistive technologies: state-of-the-art and challenges, Frontiers in Neuroscience 4 (2010) 161. doi:https://doi.org/10.3389/fnins.2010.00161.

[6] R. Leeb, S. Perdikis, L. Tonin, A. Biasiucci, M. Tavella, M. Creatura, A. Molina, A. Al-Khodairy, T. Carlson, J. dR Millán, Transferring brain–computer interfaces beyond the laboratory: successful application control for motor-disabled users, Artificial intelligence in medicine 59 (2) (2013) 121–132. doi:https://doi.org/10.1016/j.artmed.2013.08.004.

[7] K.-R. Mller, M. Tangermann, G. Dornhege, M. Krauledat, G. Curio, B. Blankertz, Machine learning for real-time single-trial eeg-analysis: From braincomputer interfacing to mental state monitoring, Journal of Neuroscience Methods 167 (1) (2008) 82 – 90, brain-Computer Interfaces (BCIs). doi:https://doi.org/10.1016/j.jneumeth.2007.09.022.

[8] T. Li, J. Hong, J. Zhang, F. Guo, Brainmachine interface control of a manipulator using small-world neural network and shared control strategy, Journal of Neuroscience Methods 224 (2014) 26 – 38. doi:https://doi.org/10.1016/j.jneumeth.2013.11.015.

[9] A. Chowdhury, Y. K. Meena, H. Raza, B. Bhushan, A. K. Uttam, N. Pandey, A. A. Hashmi, A. Bajpai, A. Dutta, G. Prasad, Active physical practice followed by mental practice using bci-driven hand exoskeleton: A pilot trial for clinical effectiveness and usability, IEEE Journal of Biomedical and Health Informatics 22 (6) (2018) 1786–1795. doi:10.1109/JBHI.2018.2863212.

[10] J. Liu, P. Zhou, A novel myoelectric pattern recognition strategy for hand function restoration after incomplete cervical spinal cord injury, IEEE Transactions on Neural Systems and Rehabilitation Engineering 21 (1) (2013) 96–103. doi:https://doi.org/10.1109/TNSRE.2012.2218832.

[11] N. S. Makowski, J. S. Knutson, J. Chae, P. E. Crago, Control of robotic assistance using poststroke residual voluntary effort, IEEE Transactions on Neural Systems and Rehabilitation Engineering 23 (2) (2015) 221–231. doi:https://doi.org/10.1109/TNSRE.2014.2364273.

[12] A. Chowdhury, H. Raza, Y. K. Meena, A. Dutta, G. Prasad, Online covariate shift detection based adaptive brain-computer interface to trigger hand exoskeleton feedback for neuro-rehabilitation, IEEE Transactions on Cognitive and Developmental Systems (2018) 1–1doi:10.1109/TCDS.2017.2787040.

[13] T. M. Vaughan, J. R. Wolpaw, E. Donchin, Eeg-based communication: prospects and problems, IEEE transactions on rehabilitation engineering 4 (4) (1996) 425–430. doi:https://doi.org/10.1109/86.547945.

[14] H. Raza, D. Rathee, S. Zhou, H. Cecotti, G. Prasad, Covariate shift estimation based adaptive ensemble learning for handling non-stationarity in motor imagery related eeg-based brain-computer interface, arXiv:1805.01044 [cs.LG].
URL https://arxiv.org/abs/1805.01044

[15] T. Sadoyama, T. Masuda, H. Miyano, Relationships between muscle fibre conduction velocity and frequency parameters of surface emg during sustained contraction, European Journal of Applied Physiology and Occupational Physiology 51 (2) (1983) 247–256. doi:https://doi.org/10.1007/BF00455188.

[16] C. Brunner, B. Z. Allison, D. J. Krusienski, V. Kaiser, G. R. Müller-Putz, G. Pfurtscheller, C. Neuper, Improved signal processing approaches in an offline simulation of a hybrid brain-computer interface, Journal of Neuroscience Methods 188 (1) (2010) 165–173. doi:https://doi.org/10.1016/j.jneumeth.2010.02.002.

[17] G. R. Müller-Putz, C. Breitwieser, M. Tangermann, M. Schreuder, M. Tavella, R. Leeb, F. Cincotti, F. Leotta, C. Neuper, Tobi hybrid bci: principle of a new assistive method, Int. J. Bioelectromagn 13 (2011) 144–145.

[18] B. Allison, R. Leeb, C. Brunner, G. Müller-Putz, G. Bauernfeind, J. Kelly, C. Neuper, Toward smarter bcis: extending bcis through hybridization and intelligent control, Journal of Neural Engineering 9 (1) (2011) 013001. doi:https://doi.org/10.1088/1741-2560/9/1/013001.

[19] L. Cao, et al., A hybrid brain computer interface system based on the neurophysiological protocol and brain-actuated switch for wheelchair control, Journal of Neuroscience Methods 229 (2014) 33–43. doi:https://doi.org/10.1016/j.jneumeth.2014.03.011.

[20] M. Wang, I. Daly, B. Z. Allison, J. Jin, Y. Zhang, L. Chen, X. Wang, A new hybrid bci paradigm based on p300 and ssvep, Journal of Neuroscience Methods 244 (2015) 16 – 25. doi:https://doi.org/10.1016/j.jneumeth.2014.06.003.

[21] E. A. Kirchner, M. Tabie, Closing the gap: combined EEG and EMG analysis for early movement prediction in exoskeleton based rehabilitation, in: Proceedings of the 4th European Conference on Technically Assisted Rehabilitation-TAR 2013, 2013.

[22] P. Xie, X. Chen, P. Ma, X. Li, P. Su, Identification method of human movement intention based on the fusion feature of EEG and EMG, in: Proceedings of the World Congress on Engineering, Vol. 2, 2013.

[23] N. A. Bhagat, A. Venkatakrishnan, B. Abibullaev, E. J. Artz, N. Yozbatiran, A. A. Blank, J. French, C. Karmonik, R. G. Grossman, M. K. O'Malley, et al., Design and optimization of an eeg-based brain machine interface (bmi) to an upper-limb exoskeleton for stroke survivors, Frontiers in neuroscience 10. doi:https://doi.org/10.3389/fnins.2016.00122.

[24] F. Cincotti, F. Pichiorri, P. Aricò, F. Aloise, F. Leotta, F. de Vico Fallani, J. d. R. Millán, M. Molinari, D. Mattia, EEG-based Brain-Computer Interface to support post-stroke motor rehabilitation of the upper limb, in: 2012 Annual International Conference of the IEEE Engineering in Medicine and Biology Society, IEEE, 2012, pp. 4112–4115. doi:https://doi.org/10.1109/EMBC.2012.6346871.

[25] J. Rouillard, A. Duprès, F. Cabestaing, S. Leclercq, M.-H. Bekaert, C. Piau, J.-M. Vannobel, C. Lecocq, Hybrid bci coupling eeg and emg for severe motor disabilities, Procedia Manufacturing 3 (2015) 29–36. doi:https://doi.org/10.1016/j.promfg.2015.07.104.

[26] R. Leeb, H. Sagha, R. Chavarriaga, J. del R Millán, A hybrid brain–computer interface based on the fusion of electroencephalographic and electromyographic activities, Journal of neural engineering 8 (2) (2011) 025011. doi:https://doi.org/10.1088/1741-2560/8/2/025011.

[27] Y. Hashimoto, J. Ushiba, A. Kimura, M. Liu, Y. Tomita, Correlation between EEG-EMG coherence during isometric contraction and its imaginary execution, Acta Neurobiol Exp (Wars) 70 (1) (2010) 76–85.

[28] T. Shibata, Y. Suhara, T. Oga, Y. Ueki, T. Mima, S. Ishii, Application of multivariate autoregressive modeling for analyzing the interaction between eeg and emg in humans, in: International Congress Series, Vol. 1270, Elsevier, 2004, pp. 249–253. doi:https://doi.org/10.1016/j.ics.2004.05.048.

[29] B. Conway, D. Halliday, S. Farmer, U. Shahani, P. Maas, A. Weir, J. Rosenberg, Synchronization

between motor cortex and spinal motoneuronal pool during the performance of a maintained motor task in man, The Journal of physiology 489 (Pt 3) (1995) 917.

[30] D. M. Halliday, B. A. Conway, S. F. Farmer, J. R. Rosenberg, Using electroencephalography to study functional coupling between cortical activity and electromyograms during voluntary contractions in humans, Neuroscience letters 241 (1) (1998) 5–8. doi:https://doi.org/10.1016/S0304-3940(97)00964-6.

[31] T. Mima, K. Toma, B. Koshy, M. Hallett, Coherence between cortical and muscular activities after subcortical stroke, Stroke 32 (11) (2001) 2597–2601.

[32] Y. Fang, J. J. Daly, J. Sun, K. Hvorat, E. Fredrickson, S. Pundik, V. Sahgal, G. H. Yue, Functional corticomuscular connection during reaching is weakened following stroke, Clinical neurophysiology 120 (5) (2009) 994–1002. doi:https://doi.org/10.1016/j.clinph.2009.02.173.

[33] W. Omlor, L. Patino, M.-C. Hepp-Reymond, R. Kristeva, Gamma-range corticomuscular coherence during dynamic force output, Neuroimage 34 (3) (2007) 1191–1198. doi:https://doi.org/10.1016/j.neuroimage.2006.10.018.

[34] R. Kristeva-Feige, C. Fritsch, J. Timmer, C.-H. Lücking, Effects of attention and precision of exerted force on beta range eeg-emg synchronization during a maintained motor contraction task, Clinical Neurophysiology 113 (1) (2002) 124–131. doi:https://doi.org/10.1016/S1388-2457(01)00722-2.

[35] Q. Yang, V. Siemionow, W. Yao, V. Sahgal, G. H. Yue, Single-trial eeg-emg coherence analysis reveals muscle fatigue-related progressive alterations in corticomuscular coupling, IEEE transactions on neural systems and rehabilitation engineering 18 (2) (2010) 97–106. doi:https://doi.org/10.1109/TNSRE.2010.2047173.

[36] X. Lou, S. Xiao, Y. Qi, X. Hu, Y. Wang, X. Zheng, Corticomuscular coherence analysis on hand movement distinction for active rehabilitation, Computational and mathematical methods in medicine 2013. doi:http://sci-hub.tw/10.1155/2013/908591.

[37] G. Severini, S. Conforto, M. Schmid, T. D'Alessio, A multivariate auto-regressive method to estimate cortico-muscular coherence for the detection of movement intent, Applied Bionics and Biomechanics 9 (2) (2012) 135–143. doi:http://sci-hub.tw/10.3233/ABB-2011-0036.

[38] Z. Bayraktaroglu, K. von Carlowitz-Ghori, F. Losch, G. Nolte, G. Curio, V. V. Nikulin, Optimal imaging of cortico-muscular coherence through a novel regression technique based on multi-channel eeg and un-rectified emg, NeuroImage 57 (3) (2011) 1059–1067. doi:http://sci-hub.tw/10.1016/j.neuroimage.2011.04.071.

[39] G. Pfurtscheller, B. Graimann, J. E. Huggins, S. P. Levine, L. A. Schuh, Spatiotemporal patterns of beta desynchronization and gamma synchronization in corticographic data during self-paced movement, Clinical neurophysiology 114 (7) (2003) 1226–1236. doi:https://doi.org/10.1016/S1388-2457(03)00067-1.

[40] D. Tuncel, A. Dizibuyuk, M. K. Kiymik, Time frequency based coherence analysis between eeg and emg activities in fatigue duration, Journal of medical systems 34 (2) (2010) 131–138. doi:https://doi.org/10.1007/s10916-008-9224-y.

[41] A. Chwodhury, H. Raza, A. Dutta, S. S. Nishad, A. Saxena, G. Prasad, A study on cortico-muscular coupling in finger motions for exoskeleton assisted neuro-rehabilitation, in: 2015 37th Annual International Conference of the IEEE Engineering in Medicine and Biology Society (EMBC), IEEE, 2015, pp. 4610–4614. doi:https://doi.org/10.1109/EMBC.2015.7319421.

[42] S. F. Farmer, et al., The frequency content of common synaptic inputs to motoneurones studied during voluntary isometric contraction in man, The Journal of Physiology 470 (1) (1993) 127–155. doi:https://doi.org/10.1113/jphysiol.1993.sp019851.

[43] Y. K. Meena, A. Chowdhury, H. Cecotti, K. Wong-Lin, S. S. Nishad, A. Dutta, G. Prasad, Emohex: An eye tracker based mobility and hand exoskeleton device for assisting disabled people, in: 2016 IEEE International Conference on Systems, Man, and Cybernetics (SMC), 2016, pp. 002122–002127. doi:10.1109/SMC.2016.7844553.

[44] A. Chowdhury, S. S. Nishad, Y. K. Meena, A. Dutta, G. Prasad, Hand-exoskeleton assisted progressive neurorehabilitation using impedance adaptation based challenge level adjustment method, IEEE Transactions on Haptics (2018) 1–1doi:10.1109/TOH.2018.2878232.

[45] T. Weiss, E. Hansen, L. Beyer, M.-L. Conradi, F. Merten, C. Nichelmann, R. Rost, C. Zippel, Activation processes during mental practice in stroke patients, International Journal of Psychophysiology 17 (1) (1994) 91 – 100. doi:http://dx.doi.org/10.1016/0167-8760(94)90059-0.

[46] O. T., Brain-computer interface with somatosensory feedback improves functional recovery from severe hemiplegia due to chronic stroke, Frontiers in Neuroengineering 7 (19) (2014) 1–7. doi:https://doi.org/10.3389/fneng.2014.00019.

[47] J. J. Daly, et al., Feasibility of a new application of noninvasive brain computer interface (bci): A case study of training for recovery of volitional motor control after stroke, Journal of Neurologic Physical Therapy 33 (4) (2009) 203–211. doi:https://doi.org/10.1097/NPT.0b013e3181c1fc0b.

[48] R. C. Lyle, A performance test for assessment of upper limb function in physical rehabilitation treatment and research, International Journal of Rehabilitation Research 4 (4) (1981) 483–492.

[49] B. Kim, L. Kim, Y.-H. Kim, S. K. Yoo, Cross-association analysis of eeg and emg signals according to movement intention state, Cognitive Systems Research 44 (2017) 1 – 9. doi:https://doi.org/10.1016/j.cogsys.2017.02.001.

[50] J. Rosenberg, A. Amjad, P. Breeze, D. Brillinger, D. Halliday, The fourier approach to the identification of functional coupling between neuronal spike trains, Progress in biophysics and molecular biology 53 (1) (1989) 1–31.

[51] P. Belardinelli, et al., Plasticity of premotor cortico-muscular coherence in severely impaired stroke patients with hand paralysis, Neuroimage Clin. 16 (14) (2017) 726–733. doi:10.1016/j.nicl.2017.03.005.

[52] D. J. Hewson, et al., Feasibility of a new application of noninvasive brain computer interface (bci): A case study of training for recovery of volitional motor control after stroke, Journal of Electromyography and Kinesiology 13 (3) (2003) 273–279. doi:https://doi.org/10.1097/NPT.0b013e3181c1fc0b.

[53] A. G. Androulidakis, L. M. Doyle, K. Yarrow, V. Litvak, T. P. Gilbertson, P. Brown, Anticipatory changes in beta synchrony in the human corticospinal system and associated improvements in task performance, European Journal of Neuroscience 25 (12) (2007) 3758–3765. doi:https://doi.org/10.1111/j.1460-9568.2007.05620.x.

[54] S. W. Tung, C. Guan, K. K. Ang, K. S. Phua, C. Wang, C. W. K. Kuah, K. S. G. Chua, Y. S. Ng, L. Zhao, E. Chew, A measurement of motor recovery for motor imagery-based bci using eeg coherence analysis, in: 2015 10th International Conference on Information, Communications and Signal Processing (ICICS), IEEE, 2015, pp. 1–5. doi:https://doi.org/10.1109/ICICS.2015.7459816.

[55] R. Pineiro, S. Pendlebury, H. Johansen-Berg, P. Matthews, Functional mri detects posterior shifts in primary sensorimotor cortex activation after stroke evidence of local adaptive reorganization?, Stroke 32 (5) (2001) 1134–1139. doi:https://doi.org/10.1161/01.str.32.5.1134.